Pergamon

PII: S0042-6989(97)00286-1

Vision Res., Vol. 38, No. 5, pp. 627–635, 1998

Printed in Great Britain
0042-6989/98 $19.00 + 0.00

Rod Photoresponses in 6-week and 4-month-old Human Infants

S. NUSINOWITZ,*§ D. G. BIRCH,†‡ E. E. BIRCH†‡

Received 31 January 1997; in revised form 19 August 1997

Rod-only electroretinograms (ERGs) were recorded from 6-week and 4-month-old normal human infants. The leading edge of the rod *a*-wave was fitted with a model of the activation phase of phototransduction to provide estimates of *S* (a sensitivity parameter) and Rm_{P3} (the maximum saturated photoreceptor response) at each of the investigated ages. Both *S* and Rm_{P3} increased over the first postnatal months but followed different developmental time courses with *S* approaching adult-like values sooner than Rm_{P3}. The changes in *S* and Rm_{P3} can be interpreted within the context of a model incorporating the combined effects of increased levels of rhodopsin and the changing structure of the rod outer segment during development. © 1998 Elsevier Science Ltd. All rights reserved.

Rods Infants Photoresponses Electroretinography

INTRODUCTION

Large increases in scotopic sensitivity have been observed over the first postnatal months using behavioral measures (Brown, 1986, 1988; Hamer & Schneck, 1984; Hansen, Fulton, & Harris, 1986; Powers, Schneck, & Teller, 1981). Powers *et al.* (1981), for example, used a forced-choice preferential looking technique to measure infants' dark-adapted thresholds. They reported that thresholds for infants were 50-times greater than adults' at 1 month and 10-times greater at 3 months of age, a shift of approximately 0.70 log unit over the first postnatal months. Although localizing the sites of these developmental changes has been the focus of much debate (see, for example, Brown, 1990; Hood, 1988; Fulton & Hansen, 1992; Hood, Birch, & Birch, 1993a), it is generally accepted that at least part of the improvement in scotopic sensitivity observed behaviorally occurs within the retina, largely due to maturation at the receptoral level (Hood, 1988; Hood *et al.*, 1993a).

The contribution made by the developing retina to improved scotopic sensitivity has been studied using the electroretinogram (ERG). As with behavioral measures, the ERG undergoes substantial improvement over the first postnatal months (Birch, Birch, Petrig, & Uauy, 1990; Birch, Birch, & Uauy, 1991; Birch, Birch, Hoffman, & Uauy, 1992; Breton, Quinn, & Schueller, 1995; Fulton & Hansen, 1982, 1985). However, much of the work on the development of the ERG has focused on the trough-to-peak amplitude of the rod *b*-wave. Trough-to-peak *b*-wave amplitude reflects the sum of potentials of opposite polarity generated by the rod photoreceptors and by cells of the inner retina, presumably the Muller and bipolar cells of the inner nuclear layer (INL). Changes in *b*-wave amplitude cannot specifically indicate the contributions made by each retinal site; immaturities in either the photoreceptor or the inner retina could have the same effects on *b*-wave amplitude (Hood *et al.*, 1993a).

Photoreceptor function can be studied directly using the *a*-wave of the ERG, which is known to be generated within the photoreceptor layer (Granit, 1935, 1955). Recent advances in the analysis of the *a*-wave have provided a method for the quantitative assessment of photoreceptor function (Hood & Birch, 1990a,b, 1991; Breton & Montzka, 1992; Cideciyan & Jacobson, 1993; Breton, Schueller, Lamb, & Pugh, 1994). Thus, immaturities in infant vision that originate at the level of the photoreceptor can now be studied relatively independently of other layers of the retina by examining the changes with age in the parameters derived from the analysis of the *a*-wave.

Fulton and Hansen (1992) recorded *a*-waves from 10-week-old infants and adult controls and analyzed these waveforms using an early version of a rod model (Hood & Birch, 1990a). Median dark-adapted sensitivity (defined as the intensity producing a semi-saturated *a*-wave) was 0.36 log unit lower for infants compared with adults. However, only a single time point was investigated for infants and age-related trends could not be evaluated. More recently, Breton *et al.* (1995) applied a

*Jules Stein Eye Institute, 100 Stein Plaza, Los Angeles, CA 90024, U.S.A.
Retina Foundation of the Southwest, 9900 N. Central Expressway, Suite 400, Dallas, TX 75231, U.S.A.
‡Department of Ophthalmology, University of Texas Southwestern Medical School, Dallas, TX 75235, U.S.A.
§To whom all correspondence should be addressed: [*Fax*: 310 206 3652; *Email*: nusinowitz@jsei.ucla.edu].

rod model (Breton *et al.*, 1994) to infant data and reported that both the amplification constant (gain) of transduction and the maximum saturated response are immature at birth, and increase roughly in parallel, reaching mature values at approx. 5 years of age or older. However, in their study, only nine infants were less than 4 months of age and only 16 were less than 1 year of age. In addition, the youngest infants were patients referred for clinical evaluation and they were included in the study if, on the basis of an ophthalmological examination, the retina was deemed normal. This selection bias does not preclude the possibility of sub-clinical pathology in these young patients.

In this study, photoresponses of rods in 6-week and 4-month-old infants were derived from the *a*-wave of the ERG. As a departure from earlier work, a relatively large number of infants was represented at the selected ages and all infants had normal visual function. The leading edge of the rod *a*-wave for each infant was fitted with a current model of the activation phase of phototransduction (Hood & Birch, 1993, 1994) to provide parameters of rod function.

METHODS

Subjects

Normal healthy infants, born 37–41 weeks postconception, with no family history of eye disease and a normal neonatal ophthalmic examination, were recruited from local pediatric practices. Electroretinograms were obtained from 14 6-week-old infants (mean age ± 1 standard deviation = 43 ± 7 days) and 15 4-month-old infants (mean age ± 1 standard deviation = 124 ± 3 days). Electroretinograms were also obtained from 20 normal adults (mean age ± 1 standard deviation = 33 ± 14 years) for comparison. The tenets of the Declaration of Helsinki were adhered to. Written consent was obtained from the parents of each infant after the goals of the study were explained and the potential risks and benefits were described.

Recording techniques

The methods used for obtaining full-field ERGs were relatively standard. One eye was dilated (0.2% cyclopentolate hydrochloride and 1% phenylephrine hydrochloride) and dark-adapted. Responses were obtained from the anesthetized cornea using a pediatric-size Burian-Allen bipolar contact lens (Hansen Ophthalmic, Iowa City, IA). Responses were amplified (gain = 10 000; 3 dB down at 2 and 300 Hz) and acquired through an A/D converter (National Instruments, Austin, TX) in a personal computer. Signals were averaged as described below.

Apparatus and stimuli

All stimuli were presented in a Ganzfeld dome whose interior surface was painted with a highly reflective white matte paint (Eastman Kodak Corporation, #6080). Two separate domes were constructed. One dome was attached to a frame that was designed to permit lowering of the dome over the head of a supine infant. An identical dome, designed for adults, was affixed upright on a table in a standard way. All stimuli (1.3 msec in duration) were derived from a circular Xenon gas flash tube (Novatron Inc. of Dallas) driven by a 1600w power supply. The flash head was affixed to the outside of the dome in a light tight housing. An opening in the dome below the flash head and positioned at 90 deg to the viewing porthole allowed light to penetrate the interior of the dome.

Short-wavelength ("blue") flashes with ultraviolet light blocked (Wratten 47B; λ_{max} = 449 nm + Wratten HF-3) were varied in 0.3 log unit steps from approximately 3.2 up to 4.2 log scotopic td-sec. Typically, four intensities were delivered and no infant was presented with fewer than three intensities. Thus, the intensity range examined was varied by a factor of 8–10 depending on the level of co-operation of the particular infant (see below).

In the dark-adapted state, responses to the blue flashes are primarily rod-driven (Hood & Birch, 1990a,b, 1994). Nevertheless, the responses also contain a small cone component. The cone component was isolated either by recording *a*-waves to long-wavelength (W26; λ_{cut-on} = 605 nm) "red" flashes that were photopically matched to the blue intensity series or by recording *a*-waves to the same blue intensity series on a rod saturating background. (The latter method was used primarily for the infants.) For both methods, a white background with an intensity of 1.80 log photopic cd/m^2 (2.17 log scotopic cd/m^2) was used to suppress rod function. Rod-only ERGs were derived by computer-subtracting the "cone" component from the responses to dark-adapted blue flashes. Evidence that the two procedures remove cone contributions and produce indistinguishable rod-isolated ERGs has been presented (Hood & Birch, 1993; Pepperberg, Birch, & Hood, 1997).

Procedure

All infants and adults were dark-adapted for 40 min prior to testing. Infants were placed supine in a car seat and swaddled to prevent arm movements. Soft foam rubber blocks were positioned on either side of the head to restrict head movements. The contact lens electrode was inserted under dim red light and the Ganzfeld dome was lowered over the infant's head. Eye position was monitored by an observer who viewed the infant through a small hole positioned at the equator opposite the viewing porthole. For the dark-adapted conditions, a dim red LED (light-emitting diode) positioned on the inside of the dome provided sufficient light to monitor eye position. For the light-adapted conditions, the background light provided illumination. The recording of responses was triggered only when a pupil was visible and centered within the contact lens electrode. Adults were seated in front of the dome and were instructed to fixate a small red LED positioned on the inside surface opposite the viewing porthole. A chin- and headrest were provided to maintain head position. For both infants and

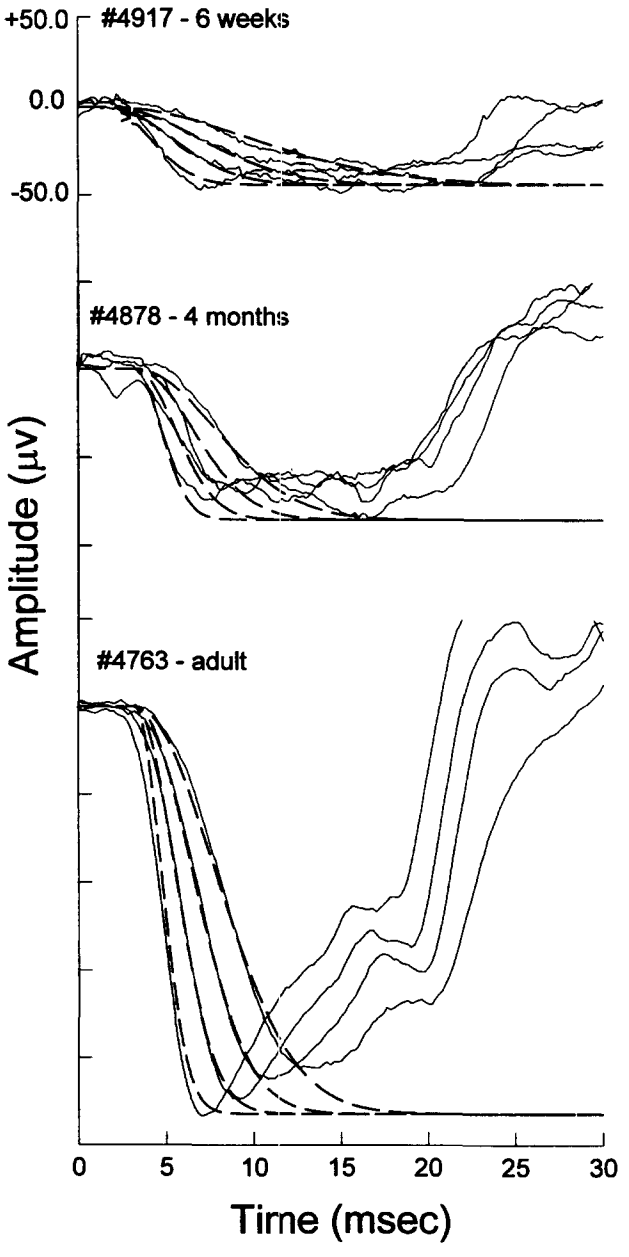

FIGURE 1. Representative ERG recordings to a range of flash intensities for 6-week-old (top panel) and 4-month-old infants (middle panel), and a normal adult (bottom panel). Retinal illuminance was varied in 0.3 log unit steps from 3.1 to 4.0 log scot td-sec for infant #4917, from 3.2 to 4.1 log scot td-sec for infant #4878, and from 3.5 to 4.4 log scot td-sec for adult #4763. The irregular wavy curves are the raw data and the smooth dashed curves are the fit of equation (1) obtained by estimation of a single set of parameters for each series of responses (the ensemble fit). In fitting equation (1), t_d was held constant at 3.2 msec, the average value for adults, and each record was truncated at the point were the *b*-wave begins to intrude, indicated by the reversal of direction of the tracing. Parameter estimates (log S $(\text{sec}^{-2}(\text{td-sec})^{-1})$ and log $|Rm_{P3}$ $(\mu V)|$) derived from the fit of equation (1) are 0.53 and 1.65 for infant #4917, 0.99 and 1.93 for infant #4878, and 0.92 and 2.36 for adult #4763.

adults, the position of the head with respect to the viewing porthole was approximately the same.

Dark-adapted responses to the blue flashes were recorded first. Three to five responses were typically averaged at each flash intensity with sufficient time between flash presentations to ensure complete recovery of rod function. An individual infant might, for example, be presented with as many as 20 flashes in the dark-adapted state (five presentations of four intensities) with approximately 30 sec between flashes (a total of approx. 10 min). However, infants were typically unco-operative during testing and this sometimes precluded recording multiple responses at the same intensity, resulting in somewhat noisier signals for infants compared with adults. Responses that were contaminated by eye-movement and muscle artifacts were repeated.

After the dark-adapted responses had been collected, a background light inside the dome was turned on and subjects were allowed to light adapt for at least 5 min. Light-adapted cone responses to the "red" or "blue" flashes were recorded using the same procedure as for the dark-adapted responses. Total testing time for infants was approximately 20–25 min.

Analysis of rod a-waves

Based on the Lamb and Pugh (1992) model of phototransduction, Hood and Birch (1993, 1994) define the leading edge of the *a*-wave by:

$$P3(i,t) \cong \{1 - \exp[-i \cdot S \cdot (t - t_d)^2]\} \cdot Rm_{P3} \quad \text{for } t > t_d, \tag{1}$$

where $P3$ is the sum of the responses of the individual rods. The amplitude, $P3$, is a function of flash energy, i, and time, t, after flash onset. S is a sensitivity parameter that scales flash energy i and Rm_{P3} is the maximum saturated photovoltage. The parameter, t_d, is a brief delay before response onset. For brief flashes, prior research has shown that equation (1) provides good fits to human rod *a*-waves (Hood & Birch, 1993, 1994) and to the photocurrent data of single human rod cells (Kraft, Schneeweis, & Schnapf, 1993).

The leading edge of the *a*-wave of the rod-isolated responses obtained for infants and adults of this study were fit with equation (1). For the purposes of analysis, each ERG recording was truncated at the point were the *b*-wave clearly intruded, indicated by the reversal of direction of the ERG tracing (see Fig. 1). In fitting the leading edge of the *a*-wave for infants, t_d was held constant at the average value of 3.2 msec obtained for the 20 adults tested. The decision to hold t_d constant was made because better fits were frequently obtained when only S and Rm_{P3} were allowed to vary. For each subject, equation (1) was fit simultaneously to the averaged responses to all intensities using a least-squares minimization procedure (Matlab, Mathworks, Natick, MA). This procedure provided a single estimate for the parameters S and Rm_{P3} for the ensemble of responses. Hereafter, all references to the parameters S and Rm_{P3} will be those determined from the ensemble fit. Prior research with adults has demonstrated that over the particular intensity range of this study, S obtained from the fit of equation (1) to individual responses (intensities), is approximately constant and not different from the value of S obtained when several intensities are fitted

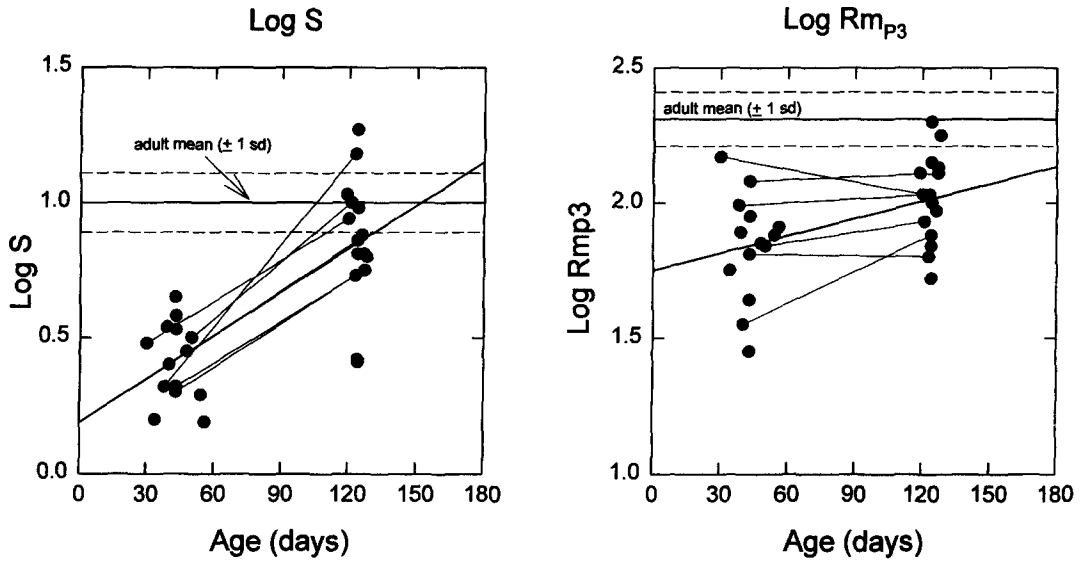

FIGURE 2. Age-related changes in log S (left panel) and log Rm_{P3} (right panel) over the first 4 months of life. The sold circles represent the parameter estimates at each age for a particular infant. The unconnected points in each graph are different infants. The points connected by solid lines are the data collected on the same infant at 6 weeks and at 4 months of age. The horizontal lines show the adult mean (solid line) and standard deviations (dashed lines) for each parameter. The solid diagonal line is a linear regression through the data at each age and is included as a visual aid to compare the rates of change in the parameters from 6 weeks to 4 months of age.

simultaneously (Hood & Birch, 1994; see also Breton *et al.*, 1994).

Retinal illuminance and correction for eye size

Retinal illuminance was calculated using a standard technique (Wyszecki & Stiles, 1982)*. In computing retinal illuminance, pupil size was measured individually for all infants and adults. We also included an additional correction for eye size. Retinal illuminance varies inversely with the square of the posterior nodal distance. Although, it was not possible to measure eye size for each infant, the physical characteristics of the infant eye, measured using ultrasonography, have been reported previously (Larson, 1971; Blomdahl, 1979). At 6 weeks of age, the axial length of the eye is approximately 17.2 mm, and at 4 months of age, it is approx. 19.4 mm. The axial length of a normal adult eye is approximately 23 mm. Based on these measures of eye size, we assumed that stimuli presented to the eye of 6-week and 4-month-old infants were 0.25 and 0.15 log units, respectively, more effective than the same stimuli calibrated for the adult eye.

RESULTS

Rod a-waves for a representative 6-week and 4-month-old infant are shown in the Fig. 1(top and middle panels). For comparison, rod a-waves for a normal adult are shown in Fig. 1(bottom panel). The smooth dashed lines through each set of responses are the fit of equation (1) obtained by estimating a single set of parameters for all of the responses (the ensemble fit). Each record was truncated at the point where the b-wave begins to intrude, indicated by the reversal of direction of the tracing (solid lines). For the representative subjects shown in Fig. 1, the maximal a-wave response, Rm_{P3} (μV), increases with age. Log Rm_{P3} at 6 week [Fig. 1(top panel)] is 1.65 and at 4 months [Fig. 1(middle panel)] is 1.93 μV. Log Rm_{P3} for the representative adult is 2.36 μV. The parameter S (sec^{-2}(td-sec)$^{-1}$) also increases from 6 weeks to 4 months, but appears relatively adult-like at 4 months. For the subjects shown in Fig. 1, log S is 0.53, 0.99, and 0.92, respectively.

Between-group comparisons

Figure 2 summarizes the age-related changes in S [Fig. 2(left panel)] and Rm_{P3} [Fig. 2(right panel)] that occurred over the first 4 months for the infants of this study. (The data points that are connected by thin solid lines are repeated measures on the same subject. Their data will be described separately below.) Despite some variability at each age, there is a clear developmental trend—both S and Rm_{P3} improve with age. On average, log S at 6 weeks is 0.41 (±0.14) and at 4 months is 0.86 (±0.24), a shift of 0.45 log unit ($t = 6.24$, df = 23, $P < 0.001$). Correspondingly, log Rm_{P3} improves by approx. 0.18 log unit from 1.84 (±0.20) at 6 weeks to 2.02 (±0.17) at 4 months ($t = 2.64$, df = 27, $P < 0.014$). Thus, both S and Rm_{P3} improve with age, but the rate of improvement, as indexed by the slope of the solid diagonal line through each dataset (assuming a linear progression, but see Fig. 5), is greater for S than for Rm_{P3}.

The data are shown in a different form in Fig. 3(left and

*We measured each flash in units of photopic cd/m^2-sec. The conversion from photopic to scotopic effectiveness was 1.35 (Hood & Birch, 1994). Retinal illuminance is given by the relation $t_S = L_S \times A$, where t_S = retinal illuminance, L_S = scotopic luminance (cd/m^2-sec), and A = pupil area (mm^2) (Wyszecki & Stiles, 1982).

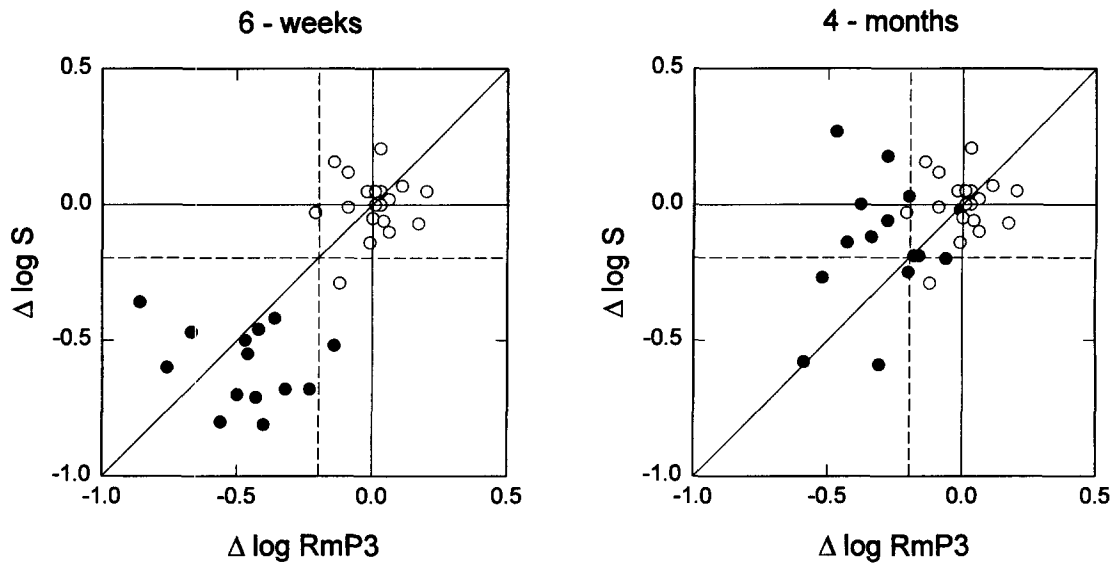

FIGURE 3. Departures from adult estimates for log S and log Rm_{P3} at 6 weeks (left panel) and 4 months (right panel) of age. Changes in log S and log Rm_{P3} are expressed as the differences (Δlog S and Δlog Rm_{P3}) from the log of the mean of adult controls. A value of 0.0 corresponds to the mean of the adult value (a departure score of 0.0). The filled circles are the infant data and, for comparison, adult data are shown as open circles. The dashed lines are the lower boundary limits (defined as 1.96 standard deviations below the mean) for adult Δlog S (horizontal dashed line) and Δlog Rm_{P3} (vertical dashed line) of this study. The dashed lines show the values beyond which 97.5% of the adult difference scores lay for these parameters.

right panels). Here S and Rm_{P3} are expressed as the differences from the mean of adult controls. A value of 0.0 Δlog S and 0.0 Δlog Rm_{P3} corresponds to the mean of the adult value (a departure score of 0.0). The filled circles are the infant data and, for comparison, adult data are shown as open circles. The dashed lines are the lower boundary limits (defined as 1.96 standard deviations below the mean) for Δlog S (horizontal dashed line) and Δlog Rm_{P3} (vertical dashed line) obtained for the adults of this study. That is, the dashed lines show the values beyond which 97.5% of the adult difference scores lay for these parameters. Almost without exception, Δlog S and Δlog Rm_{P3} at 6 weeks fall below the lower limits for adults. By 4 months of age, the difference scores are smaller, and in some instances the parameters are within adult limits, particularly for S.

The observation that many of the older infants had log S values within adult limits, even when log Rm_{P3} is smaller, suggests that the parameter S matures more rapidly than Rm_{P3}. [The data points would be expected to

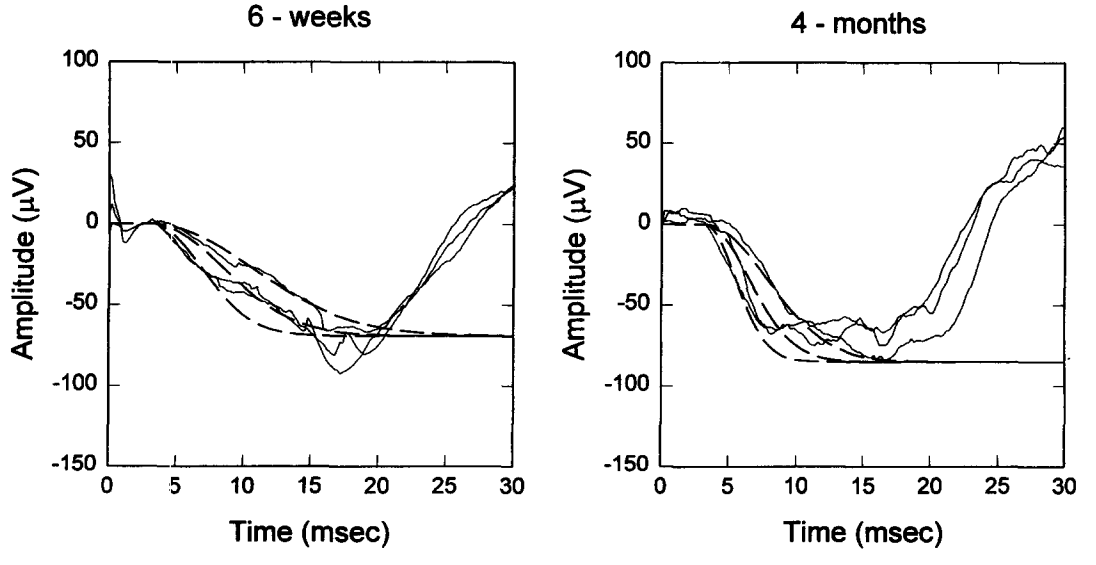

FIGURE 4. ERG a-waves recorded from the same infant (#4878) at 6 weeks (left panel) and at 4 months (right panel) of age. Retinal illuminance at both ages ranged from 3.1 to 3.8 log scot td-sec. The smooth dashed curves are the fit of equation (1) to the ensemble of responses. The data at 4 months are the same as those shown in Fig. 1(b) except that the highest intensity is not displayed. The intention was to show the progression of responses for the same intensities on one infant at both ages. Parameter estimates (log S, log Rm_{P3}) derived from the fit of equation (1) are 0.50 and 1.84, respectively, at 6 weeks and 0.99 and 1.93, respectively, at 4 months.

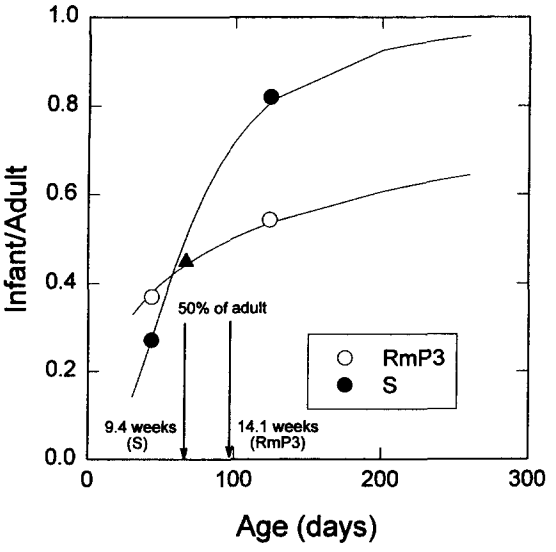

FIGURE 5. Growth curves for the parameters S (filled circles) and Rm_{P3} (open circles) as a function of age. Each data point plots the mean of the parameter estimate for infants. The smooth curves through the data points are logistic growth curves of the form $Y = Y_{max}[Age^n/(Age^n + \sigma^n)]$, where Y is the estimate for infants, Y_{max} is the estimated adult value for the parameter, and σ is the age at which $Y = Y_{max}/2$ or 50% of adult values. The logistic growth curves predict that S and Rm_{P3} are 50% of adult values at 9.4 and 14.1 weeks, respectively. The rate of progression appears slower for Rm_{P3} compared with S. The exponent, n, derived from the logistic fits, is 1.5 for S and 0.6 for Rm_{P3}. The solid triangle indicates the age at which rhodopsin content of the infant eye is 45% of adult (Fulton *et al.*, 1996).

shift along the diagonal solid line in Fig. 3(left and right panels) if the two parameters improved at the same rate.] However, at 6 weeks, log Rm_{P3} is already closer to adult values than is log S ($\Delta\log Rm_{P3}$ and $\Delta\log S$ are -0.47 and -0.59, respectively). This implies that Rm_{P3} has already matured substantially by the time that we began our experiments. However, over the time course of this experiment, S appears to mature more rapidly than Rm_{P3}. At 4 months, $\Delta\log Rm_{P3}$ and $\Delta\log S$ are -0.29 and -0.14, respectively.

Within-subjects comparisons

Six infants were tested at both 6 weeks and 4 months of age, providing repeated measures on the same infant. An example of responses obtained at 6 weeks and at 4 months for the same intensity range is shown in Fig. 4. The data at 4 months are from the same infant shown in Fig. 1(middle panel) except that the highest intensity, which was not collected at the earlier age, is not displayed. (Our intention is to show the progression of responses over the same intensity range at the two ages. Parameter estimates at 4 months were derived from all intensities and were not different from those obtained when the highest intensity was excluded.)

The data for the six infants for which there are repeated measures are shown as the thin solid lines in Fig. 2(left and right panels). The intention of this analysis is to show that the major conclusions drawn from the between-group comparisons hold within the framework of the more powerful within-subjects design. For this subgroup of infants, S increased 0.52 log unit (compared with 0.45 log unit over all infants) from 6 weeks to 4 months of age ($F = 45.8$, $P < 0.001$). Rm_{P3} increased 0.05 log unit (compared with 0.18 log unit over all infants) from 6 weeks to 4 months ($F = 0.30$, ns). At 6 weeks, $\Delta\log S$ and $\Delta\log Rm_{P3}$ are -0.63 and -0.41, respectively, and at 4 months the corresponding departures from adult values are -0.15 and -0.34.

The within-subject comparisons, therefore, support the main conclusions drawn from the between-subjects analysis described above: (1) estimates of both S and Rm_{P3} are smaller than adult values at 6 weeks and at 4 months of age; (2) both S and Rm_{P3} increase from 6 weeks to 4 months of age; and (3) Rm_{P3} is more adult-like at 6 weeks than is S, but S improves more rapidly over the time course of our experiment, reaching mature values before Rm_{P3}.

DISCUSSION

Electroretinograms to brief and relatively intense flashes of light were recorded in normal human infants at 6 weeks and 4 months of age. The leading edge of rod-isolated a-waves were fitted with a computational model of the activation phase of phototransduction to provide estimates of parameters indexing photoreceptor activity (Hood & Birch, 1993, 1994). The model provided estimates for the parameter, S (a sensitivity parameter), and Rm_{P3} (the maximum saturated photoreceptor response) at each of the ages investigated. These parameters can be used to describe immaturities in infant vision that originate at the level of the rod photoreceptor (see below). The results of this study show that both S and Rm_{P3} improve with age but follow different developmental time-courses, with S approaching adult-like values sooner than Rm_{P3} (see Figs 2 and 5).

Changes in S

Estimates for the parameter, S, derived from the fit of the rod model, are smaller in infants than in adults; S is on average 0.59 log unit less than that of adults at 6 weeks and 0.14 log unit less at 4 months of age. Within the context of the Hood & Birch (1993, 1994) rod model, S is a sensitivity parameter that scales flash energy. Thus, any factor that decreases quantal catch, or, alternatively, any factor that reduces the gain at one or more of the steps involved in phototransduction, will result in a reduction in the estimate of S.

Among the potential factors that might operate to decrease quantal catch in the infant eye are rod packing density, photoreceptor alignment, and pigment content. Rod packing density could affect quantal catch because a greater percentage of quanta would be expected to be lost in the intervening extrareceptoral space if photoreceptors were hypothesized to be less densely packed in the developing retina. This factor is unlikely to contribute substantially, since there is evidence that receptor inner segments grow to keep the interstitial space approximately constant (Packer, Hendrickson & Curcio, 1990). In addition, light reaching the rod outer segment (ROS)

depends on light-trapping, or funnelling, of light by the rod inner segments. Altered light-funnelling by inner segments as a result of receptor misalignment can operate in the direction of reducing the efficiency of quantum catch. In general, photoreceptor organization (packing density, receptor organization and alignment) can have effects in the direction of decreasing quantal catch, thereby reducing the estimate of S, but the effects are presumably small and might not be expected to carry a significant portion of the changes in sensitivity that we have observed over the first 4 months.

More significant consequences might be expected if the concentrations of rhodopsin, or other principle proteins involved in phototransduction, were immature and changing over time. Phototransduction in retinal rods is initiated by the absorption of a quanta of light by the rod pigment, rhodopsin. The photoisomerization of a single rod pigment molecule begins a series of biochemical events that ultimately leads to a decrease in the intracellular level of cyclic guanosine 3,5′-monophosphate (cGMP) and to the closure of some of the cGMP-gated channels in the plasma membrane of the outer segment. The closure of the cGMP-gated channels decreases the circulating "dark-current" and produces an electrical response—the "generator" for the ERG a-wave. (For reviews, see Baylor, Nunn & Schnapf, 1984; Pugh & Cobbs, 1986; Pugh & Lamb, 1993; Stryer, 1986.)

The infant retina is known to contain significantly less rhodopsin than the retina of an adult eye. Fulton, Dodge, Hansen, Schremser, and Williams (1991) estimate the total rhodopsin content of infant eyes to be about 1/4 and 1/2 of adult values between 32 weeks gestational age and 6 months, or approx. 0.6 and 0.3 log unit, respectively, less than that of adults. In addition, recent evidence suggests that pigment concentration (rhodopsin content per unit ROS length) is lower in the immature eye. In the developing rat retina, growth of the ROS precedes the maturation of rhodopsin content, resulting in a lower concentration of rhodopsin per rod (Fox & Rubinstein, 1989; Fulton, Hansen, & Findl, 1995). If human photoreceptor development is hypothesized to follow a qualitatively similar pattern, then it is likely that the concentration of rhodopsin in the human infant eye is also lower than in the adult eye. Recent evidence has also suggested that the concentration of mature rhodospin *per disc* is increasing with development. Using microspectrophotometric techniques to assess rhodopsin absorbance in localized regions of the rat ROS, Dodge, Fulton, Parker, Hansen, and Williams (1996) have reported a gradient of rhodopsin concentration, with the accumulation of mature rhodopsin first appearing at the base of the ROS, where new disks are continuously added, and less mature rhodopsin concentrations at the tip of the ROS.

Low rhodopsin concentration would be expected to produce a lower overall sensitivity because fewer photons can be captured by the available rhodopsin molecules. In the rat retina, Fulton, Hansen, Dorn, and Hendrickson (1996) have shown that the increase in the parameter S, obtained from an analysis of the a-wave of the ERG, is correlated to the growth curve describing age-related changes in rhodopsin content. Our results are consistent with a similar relationship in human infants. Fulton *et al.* (1996) assayed rhodopsin content in human donor eyes aged 32 weeks gestation to adulthood. A logistic growth curve (Hoglund, Nilsson, & Schwemer, 1982) fitted to the data predicts rhodopsin content to be 45% of that of adults at 10 weeks of age. We cannot explicitly define the relationship between the growth curves for S and rhodopsin content since, in this study, rod photoresponses were derived at only two ages. Nevertheless, logistic growth curves of the same form as Hoglund *et al.* (1982) can be fitted to the estimates of S. The data would predict the parameter S to be 50% of adult values at approximately 9.5 weeks (see Fig. 5). Additional data at ages distributed over the first 4 months are necessary to define more completely the relationship between rhodopsin content and S.

The photochemical evidence would suggest that the quantity of mature rhodopsin is a major limiting factor in infant scotopic sensitivity. This does not preclude the possibility of immaturities in the gain at one or more of the steps involved in phototransduction, or in other proteins integral to phototransduction. However, Ratto, Robinson, Yan, and McNaughton (1991) recorded the light response of single neonatal rat rods and found that although sensitivity was lower in the neonate rod, the gain of the light-sensitive pathway, when expressed in terms of the absolute response to a single photoisomerization, is similar in infants and adults. The low level of sensitivity was attributed to the low level of functional rhodopsin.

Changes in Rm_{P3}

The maximum saturated amplitude, Rm_{P3}, in infants is less than that of adults. At 6 weeks of age, Rm_{P3} is, on average, 0.47 log unit less than that of adults, or about 34% of adult values. By 4 months, log Rm_{P3} is 0.29 log unit less, or about 51% of adult values.

Within the context of the rod model, Rm_{P3} is proportional to the magnitude of the circulating current in the ROS membrane at the time of flash presentation (Hood & Birch, 1990a,b, 1994; Cideciyan & Jacobson, 1993). A number of factors can affect this circulating current in the developing eye, including the ionic driving force within the cell (perhaps determined by the number of mitochondria), the electrical resistance and/or leakage of the photoreceptor layer, immaturities in membrane proteins that mediate the permeability of the outer limiting membrane, and/or the density of light-sensitive channels distributed along the ROS.

For single ROSs, the amplitude of the saturated response varies linearly with the length of the outer segment (Baylor, Lamb, & Yau, 1979). For *in vivo* recordings, it is also generally accepted that the maximum saturated voltage is proportional to the total outer segment membrane (see, for example, Breton *et al.*, 1994; Hood & Birch, 1994). Prior studies have documented the changes in retinal anatomy during

normal development (Curcio, Sloan, Kalina, & Hendrickson, 1990; Hendrickson & Drucker, 1992; Packer *et al.*, 1989; 1990). ROSs increase in length in the human (Hendrickson & Drucker, 1992) and primate retina (Packer *et al.*, 1990). At birth, ROSs in the human mid-peripheral retina are approximately 30–50% the length of that of a normal adult but by 13 months of age are relatively mature—appearing (Hendrickson & Drucker, 1992). In addition, there are regional variations in the time-course of photoreceptor development (i.e., photoreceptors in the rod-ring elongate earlier than those of the more central retina) (Hendrickson & Drucker, 1992; see also Curcio & Hendrikson, 1991). The shorter ROS in the developing eye would be expected to produce a smaller maximum saturated response, assuming that other ocular and retinal factors are constant.

Clearly, the immature retina is undergoing substantial anatomical change over the first few months of life and the smaller value of Rm_{P3} for infants is due, in part, to this anatomical growth in the number and length of ROSs. However, for the developing rat retina, the saturated amplitude of the *a*-wave lags behind the growth of the ROS (Fulton *et al.*, 1995). This indicates that it is not the total membrane area that is of importance in determining signal strength, but also the availability and appropriate functioning of the machinery that ultimately drives the light-sensitive channels of the outer segment membrane (see above). For example, some reductions in Rm_{P3} can be caused by regional immaturities in amplification, or gain, sufficient to preclude the abnormal region from contributing to Rm_{P3} (Hood, Shady & Birch, 1993).

CONCLUSION

The photochemical evidence, coupled with the anatomical changes that are occurring in ROS, indicate that a relatively large increase in photopigment optical density is taking place over the developmental period of this study. We conclude that the developmental changes in *a*-wave parameters can, largely, be explained within the context of a model integrating localized changes in rhodopsin concentration and the increasing outer segment membrane.

This analysis has found a change in sensitivity on the order of 0.45 log unit owing to factors relating to rod photoreceptors alone. Psychophysically, sensitivity changes by approx. 0.75–0.80 log units from 6 weeks to 3 months (see, for example, Powers *et al.*, 1981), but behavioral thresholds are still 1.0–2.0 log units below adults' sensitivity depending on the conditions used (Powers *et al.*, 1981; Dannemiller & Banks, 1983; Hamer & Schneck, 1984; Brown, 1986, 1988; Hansen *et al.*, 1986). The differences in the results probably reflect maturation of cells and/or connections beyond the photoreceptors themselves.

REFERENCES

Baylor, D. A., Lamb, T. D. & Yau, K. W. (1979). The membrane current of single rod outer segments. *Journal of Physiology, 288*, 589–611.

Baylor, D. A., Nunn, B. J. & Schnapf, J. L. (1984). The photocurrent, noise & spectral sensitivity of rods of the monkey *Macaca fascicularis*. *Journal of Physiology (London), 357*, 575–607.

Birch, E. E., Birch, D. G., Hoffman, D. R. & Uauy, R. D. (1992). Retinal development in very low-weight infants fed diets differing in omega-3 fatty acids. *Investigative Ophthalmology and Visual Science, 33*, 2365–2376.

Birch, E. E., Birch, D. G., Petrig, B. & Uauy, R. D. (1990). Retinal and cortical function of very low birthweight infants at 36 and 57 weeks postconception. *Clinical Vision Research, 5*, 363–373.

Birch, E. E., Birch, D. G. & Uauy, R. D. (1991). Maturation of the oscillatory potential of the human electroretinogram. *Optical Society of America Technical Digest Series, 1*, 28–31.

Blomdahl, S. (1979). Ultrasonic measurements of the eye in the newborn infant. *Acta Ophthalmologica, 57*, 1048–1052.

Breton, M. E. & Montzka, D. (1992). Empirical limits of rod photocurrent component response in the electroretinogram. *Documenta Ophthalmologica, 79*, 337–361.

Breton, M. E., Quinn, G. E. & Schueller, A. W. (1995). Development of electroretinogram and rod phototransduction response in human infants. *Investigative Ophthalmology and Visual Science, 36*, 1588–1602.

Breton, M. E., Schueller, A. W., Lamb, T. W. & Pugh, E. N. Jr (1994). Analysis of ERG *a*-wave amplification and kinetics in terms of the G-protein cascade of phototransduction. *Investigative Ophthalmology and Visual Science, 35*, 295–310.

Brown, A. M. (1986). Scotopic sensitivity of the 2-month-old human infant. *Vision Research, 26*, 707–710.

Brown, A. M. (1988). Saturation of rod initiated signals in 2-month-old human infant. *Journal of the Optical Society of America, 5*, 2145–2158.

Brown, A. M. (1990). Development of visual sensitivity to light and color vision in human infants: a critical review. *Vision Research, 30*, 1159–1188.

Cideciyan, A. V. & Jacobson, S. G. (1993). Negative electroretinograms in retinitis pigmentosa. *Investigative Ophthalmology and Visual Science, 34*, 3253–3263.

Curcio, C. A. & Hendrikson, A. (1991). Organization and development of the primate photoreceptor mosaic. In N. N. Osborn & G. J. Chader (Eds), *Progress in retinal research* (pp. 90–120). Oxford: Pergamon Press.

Curcio, C. A., Sloan, K. R., Kalina, R. E. & Hendrickson, A. E. (1990). Human photoreceptor topography. *Journal of Comparative Neurology, 292*, 497–523.

Dannemiller, J. L. & Banks, M. S. (1983). The development of light adaptation in human infants. *Vision Research, 23*, 599–609.

Dodge, J., Fulton, A. B., Parker, C., Hansen, R. M. & Williams, T. P. (1996). Rhodopsin in immature rod outer segments. *Investigative Ophthalmology and Visual Science, 37*, 1951–1956.

Fox, D. A. & Rubinstein, S. D. (1989). Age-related changes in retinal sensitivity, rhodopsin content and rod outer-segment length in hooded rats following low level lead exposure during development. *Experimental Eye Research, 48*, 237–249.

Fulton, A. B., Dodge, J., Hansen, R. M., Schremser, J. L. & Williams, T. P. (1991). The quantity of rhodopsin in young human eyes. *Current Eye Research, 10*, 977–982.

Fulton, A. B. & Hansen, R. M. (1982). Background adaptation in human infants: analyses of *b*-wave responses. *Documenta Ophthalmologica Proceedings Series, 31*, 191–197.

Fulton, A. B. & Hansen, R. M. (1985). Electroretinography: application to clinical studies of infants. *Journal of Pediatric Ophthalmology and Strabismus, 22*, 252–257.

Fulton, A. B. & Hansen, R. M. (1992). The rod sensitivity of dark adapted human infants. *Current Eye Research, 11*, 1193–1198.

Fulton, A. B., Hansen, R. M. & Findl, O. (1995). The development of the rod photoresponse from dark-adapted rats. *Investigative Ophthalmology and Visual Science, 36*, 1038–1045.

Fulton, A. B., Hansen, R. M., Dorn, E. & Hendrickson, A. (1996). Development of primate rod structure and function. In Vital-Durand, F. (Ed.), *Infant vision* (pp. 33–49). Oxford: Oxford University Press.

Granit, R. (1935). Two types of retinae and their electrical responses to intermittent stimuli in light and dark adaptation. *Journal of Physiology, 85*, 421–438.

Granit, R. (1955). *Receptors and sensory perception*. New Haven: Yale University Press.

Hamer, R. D. & Schneck, M. E. (1984). Spatial summation in dark-adapted human infants. *Vision Research, 24*, 77–85.

Hansen, R. M., Fulton, A. B. & Harris, S. J. (1986). Background adaptation in human infants. *Vision Research, 26*, 771–779.

Hendrickson, A. & Drucker, D. (1992). The development of parafoveal and rod-ring human retina. *Behavioral Brain Research, 49*, 21–31.

Hoglund, G., Nilsson, S. E. & Schwemer, J. (1982). Visual pigment and visual receptor cells in fetal and adult sheep. *Investigative Ophthalmology and Visual Science, 23*, 409–414.

Hood, D. C. (1988). Testing hypotheses about development with electroretinographic and increment-threshold data. *Journal of the Optical Society of America A, 5*, 2159–2165.

Hood, D. C. & Birch, D. G. (1990a) The a-wave of the human ERG and rod receptor function. *Investigative Ophthalmology and Visual Science, 31*, 2070–2081.

Hood, D. C. & Birch, D. G. (1990b) A quantitative measure of the electrical activity of human rod photoreceptors using electroretinography. *Visual Neuroscience, 5*, 379–387.

Hood, D. C. & Birch, D. G. (1991). Models of human rod receptors and the ERG. In M. Landy & A. Movshon (Eds), *Computational models of visual processing* (pp. 57–67). Cambridge, MA: MIT Press.

Hood, D. C. & Birch, D. G. (1993). Light adaptation of human rod receptors: the leading edge of the human *a*-wave and models of rod receptor activity. *Vision Research, 33*, 1605–1618.

Hood, D. C. & Birch, D. G. (1994). Rod phototransduction in retinitis pigmentosa: estimation and interpretation of parameters derived from the rod *a*-wave. *Investigative Ophthalmology and Visual Science, 35*, 2948–2961.

Hood, D. C., Birch, D. G. & Birch, E. E. (1993a). Use of models to improve hypothesis delineation: a study of infant electroretinography. In K. Simons (Ed.), *Early visual development, normal and abnormal* (pp. 517–535). Oxford: Oxford University Press.

Hood, D. C., Shady, S. & Birch, D. G. (1993b) Heterogeneity in retinal disease and the computational model of the human rod response. *Journal of the Optical Society of America, 10*, 1624–1630.

Kraft, T. W., Schneeweis, D. M. & Schnapf, J. L. (1993). Visual transduction in human rod photoreceptors. *Journal of Physiology, 464*, 747–765.

Lamb, T. D. & Pugh, E. N. Jr. (1992). A quantitative account of the activation steps involved in phototransduction in amphibian photoreceptors. *Journal of Physiology, 449*, 719–758.

Larson, J. S. (1971). The sagittal growth of the eye. IV. Ultrasonic measurements of the axial length of the eye from birth to puberty. *Acta Ophthalmologica, 49*, 873.

Packer, O., Hendrickson, A. E. & Curcio, C. A. (1989). Photoreceptor topography of the adult pigtail macaque *(Macaca nemestrina)* retina. *Journal of Comparative Neurology, 288*, 165–183.

Packer, O., Hendrickson, A. E. & Curcio, C. A. (1990). Developmental redistribution of photoreceptors across the *Macaca nemestrina* (pigtail macaque) retina. *Journal of Comparative Neurology, 298*, 472–493.

Pepperberg, D., Birch, D. G. & Hood, D. C. (1997). Photoresponses of human rods *in vivo* derived from paired-flash electroretinograms. *Visual Neuroscience, 14*, 73–82.

Powers, M. K., Schneck, M. S. & Teller, D. Y. (1981). Spectral sensitivity of human infants at absolute threshold. *Vision Research, 21*, 1005–1016.

Pugh, E. N. Jr. & Cobbs, W. H. (1986). Visual transduction in vertebrate rods and cones: a tale of two transmitters, calcium and cyclic GMP. *Vision Research, 26*, 1613–1643.

Pugh, E. N. Jr, Lamb, T. D. (1993). Amplification and kinetics of the activation steps in phototransduction. *Biochim. Biophys. Acta, 1141*, 111–149.

Ratto, G. M., Robinson, D. W., Yan, B. & McNaughton, P. A. (1991). Development of the light response in neonatal mammalian rods. *Nature, 351*, 654–657.

Stryer, L. (1986). The cyclic GMP cascade of vision. *Annual Review of Neuroscience, 9*, 87–119.

Wyszecki, G. & Stiles, W. S. (1982). *Color science: concepts and methods, quantitative data and formulas*. New York: Wiley.

Acknowledgements—Supported by HD22380 (Eileen E. Birch) and EY05235 (David G. Birch). We are grateful to the reviewers, and to Drs Don Hood and Bill Swanson, for helpful comments on earlier versions of the manuscript.